

Chapter 14

Photo-assisted Mineralization of the Agrochemical Pesticides Oxamyl and Methomyl and the Herbicides Diphenamid and Asulam

Hisao Hidaka, Teruo Kurihara, and Nick Serpone

Abstract Pesticides of the oximecarbamate type, such as Oxamyl and Methomyl, and the aromatic-bearing herbicides, Diphenamid and Asulam, undergo photo-assisted mineralization nearly quantitatively (ca. 90–100% within ~4 h) in aerated UV-illuminated aqueous TiO₂ dispersions. The complex structure of the agrochemicals that bear carbon, nitrogen, and sulfur functions are easily mineralized to CO₂, NH₄⁺ and NO₃⁻ ions, and SO₄²⁻ ions, respectively. Evolution of carbon dioxide has been monitored by gas chromatography and by loss of total organic carbon (TOC). The site and mode of adsorption of these agrochemicals onto the TiO₂ particle surface has been inferred from point charge calculations, whereas the position of attack by reactive oxygen species such as ·OH radicals has been estimated by frontier electron density calculations.

1 Introduction

Advanced oxidation technologies for wastewater treatment have been developed during the last two decades and are now being exploited in various industrial applications (Parsons 2004). Aquatic environments contaminated with difficult-to-biodegrade substances have become the subject of serious global concern. Some of the more promising technologies are the photo-assisted degradation methodologies that involve titanium dioxides photo-activated by Solar UV radiation despite the low content (ca. 3–5%) of the total solar flux. This lower UV irradiance impinges on the overall photon efficiencies. The highly oxidative OH

H. Hidaka (✉)

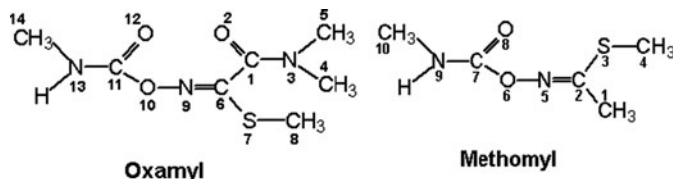
Frontier Research Center for the Global Environment Science, Meisei University,
2-1-1 Hodokubo, Hino, Tokyo 191-8506, Japan
e-mail: hidaka@epfc.meisei-u.ac.jp

and OOH radicals photogenerated on the TiO₂ surface by oxidation of water and reduction of oxygen, respectively, through charge separation under UV-irradiation attack the organic substances converting the carbon function into CO₂ gas, the sulfur into SO₄²⁻ ions, and the nitrogen function to NH₄⁺ and NO₃⁻ ions.

Photo-assisted rates of mineralization depend principally on the chemical structure of the agrochemicals examined. Rate-determining factors in the detoxification of most aquatic wastewater contaminants are their solubility in water and their mode of adsorption on the TiO₂ photo-mediator. In comparison to a hydrophilic pollutant, a hydrophobic contaminant exhibits poor adhesive properties toward the hydrophilic TiO₂ mediator, and to the extent that some agrochemical organics bearing complex functions are not commonly water-soluble, their decomposition in aqueous environments in high yields is difficult to achieve within a brief time period. As well, agrochemicals spread in fields tend to persist for relatively long periods of time without any visible decomposition. Many types of highly toxic pesticides and herbicides are typically used to exterminate vermin and other harmful insects. Within this context, the TiO₂ photo-assisted degradations of several agrochemicals such as permethrin (Hidaka et al. 1992a, b), atrazine (Pelizzetti et al. 1990; Pelizzetti et al. 2003), 2,4-dichlorophenoxyacetic acid (Watanabe et al. 2003, 2005), Diphenamid (Rahman et al. 2003), Asulam (Catastini et al. 2002a, b), paraquat (Cantavenera et al. 2006), and imazethapyr commonly used in Brazil (Ishiki et al. 2005) have been examined previously by us (Hidaka et al. 1992a, b; Watanabe et al. 2003, 2005) and by others (Pelizzetti et al. 1990, 2003; Rahman et al. 2003; Catastini et al. 2002a, b; Cantavenera et al. 2006; Ishiki et al. 2005).

Contamination of subsurface waters has recently shown increasing trends. Intake of agrochemicals by human and animals via the food chain and through drinking water, and sea and river waters has become a worrisome issue (FAO and WHO 1985; Cohen et al. 1986; Muszkat et al. 1994). Accordingly, many countries have introduced restrictive legislative regulations (EPA 2002; Dowd et al. 1988) to control and regulate the usage of these agrochemicals toward food safety since such chemicals are too often not easily biodegraded and tend to persist in nature for some time. Indeed, microbial detoxification of waters contaminated at ppm (mg L⁻¹) levels of pollutants tends to be rather difficult owing to the inefficiency of the biodegradation at such low substrate loadings (Muszkat et al. 1995) not to mention that some pollutants may also be toxic to the bacterial microorganisms.

The nitrogen- and sulfur-bearing pesticide Oxamyl is commonly used as an agrochemical in the protection of farm crops, vegetables, tobacco, and chrysanthemum among others, and is also effective in the extermination of eelworms and plant parasites (USDA 2005; Garthwaite et al. 2005). By comparison, the broad spectrum pesticide Methomyl is used (1) as an acaricide to control ticks and spiders, (2) in the foliar treatment of vegetables, fruit and field crops, cotton, and commercial ornamentals, and (3) in and around poultry houses and dairies (USDA 2005; Garthwaite et al. 2005). Note that in the structure for Oxamyl and Methomyl (and others – see below) the numbers identify the atoms for the point charge and electron density calculations.



These two pesticides belong to the class of oximecarbamates widely used to control insect and nematode pests and of which nearly 1,360 metric tons are used by the agricultural sector in the United States alone (Gianessi and Marcelli 2000). Another no less important source of pesticides in the aqueous environment is the disposal of used pesticide bottles and the rinsing of pesticide-spray containers (Malato et al. 2000). Both these carbamates inhibit the activity of the acetylcholinesterase enzyme resulting in the buildup of the neurotransmitter acetylcholine to toxic levels (Hassall 1990). Their acute toxicity ranks amongst the highest of several pesticides, thus generating some environmental concerns since both Oxamyl and Methomyl are highly water-soluble (280 g L⁻¹ and 58 g L⁻¹, respectively; Hornsby et al. 1996) and both show low affinity for adsorption onto soils (Gerstl 1984; Cox et al. 1993). This latter property renders these two carbamates highly mobile throughout the soils and aqueous ecosystems, so much so that they have been detected in groundwaters that serve as drinking waters (Kolpin et al. 2000) at concentrations that often surpass recommended thresholds (Kolpin et al. 2000; Zaki et al. 1982; Moyer and Miles 1988).

Carbamate pesticides can degrade under anoxic and abiotic conditions via a base-catalyzed elimination process to yield an oxime byproduct, methylamine and carbon dioxide. However, at pHs below 7 the process is extremely slow with half-lives of months to years (Bank and Tyrrell 1984; Chapman and Cole 1982; Harvey and Han 1978; Hegarty and Frost 1973). By contrast, a more rapid degradation occurs in an aqueous anoxic environment (e.g. a soil suspension) containing iron(II) through a two-electron reduction process generating, in addition to the oxime byproduct and methylamine, a nitrile, methanethiol, and carbon dioxide (see Fig. 1) (Strathmann and Stone 2001, 2002a, b; Bromilow et al. 1986; Smelt et al. 1983).

Others have reported the TiO₂ photo-assisted degradation of Oxamyl under direct sunlight using a compound parabolic collector system, with the pesticide being slowly mineralized to CO₂ via various non-identified intermediates subsequent to a postulated cyclization of the carbamate chain and/or ultimate cleavage of the carbamate function (Malato et al. 2000).

Diphenamid is a widely used herbicide for the control of annual broadleaf weeds such as carpetweed, chickweed, knotweed, lambs quarters, pigweed, purslane, and smartweed, as well as annual grasses. In short, it is used for the control of some broad-leaved weeds in cotton, potatoes, sweet potatoes, tomatoes, vegetables, capsicums, okra, soya beans, groundnuts, tobacco, stone fruit, citrus fruit, bush fruit, strawberries, forestry nurseries, and ornamental plants, shrubs, and trees (Elmore et al. 1968). It is also a plant growth regulator and moderately persists in the environment for about 1–3 months (Defelice 1999). Moreover, Diphenamid is

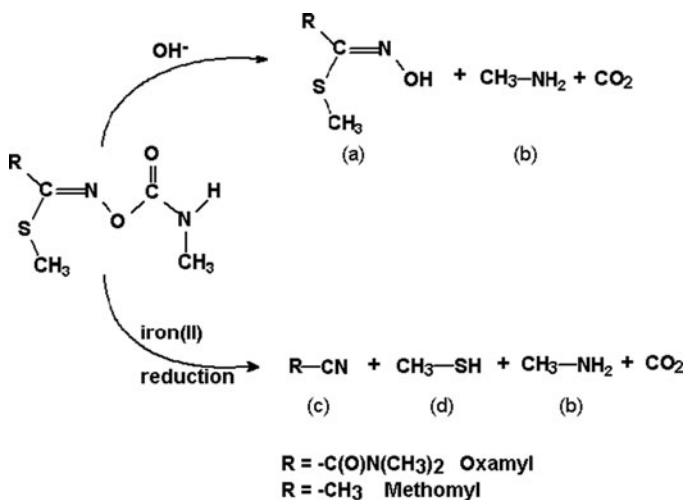
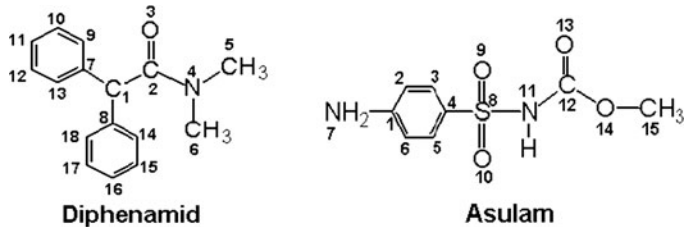


Fig. 1 Scheme illustrating the two pathways (base-catalyzed elimination and 2-electron reduction) in the degradation of the two oxime-carbamate pesticides: (a) oxime by product, (b) methylamine, (c) substituted nitrile, and (d) methanethiol. Adapted from Strathmann and Stone (2001) and from Bromilow et al. (1986)

stable to hydrolysis at pHs 5–9 for about 7–10 days at a temperature relatively higher than ambient (49°C) (Rahman et al. 2003).



The carbamate-type herbicide, Asulam, is toxic to insects and animals, and is largely used as a principal and selective herbicide in the control of bracken (Marrs et al. 1992; Bruff et al. 1995); additional details on the properties and toxicity of Asulam are available elsewhere (The International Programme on Chemical Safety (IPCS) 1996). Suffices to note that, in general, carbamate pesticides attack the nervous conveyance cell and cause abnormal excitement (IPCS 1996). This herbicide degrades photolytically faster in moist soils than in dry soils; the respective half-lives are 98 h and 350 h, respectively (Graebing et al. 2003). The photodegradation of Asulam in aqueous media in the presence of aquacomplexes as the photoinducer under sunlight irradiation necessitated from 13 to 14 h for complete degradation to CO_2 ; the principal products formed in the initial stages were parasulfanilic acid, benzoquinone, and traces of hydroquinone (Catastini et al. 2002a, b).

This article addresses the photo-assisted disposal of the pesticides Oxamyl and Methomyl and the herbicides Diphenamid and Asulam in aerated aqueous TiO_2 dispersions under bench-top UV irradiation. We show that the mineralization of these agrochemicals to carbon dioxide is nearly quantitative (ca. 90–100%) within a relatively short time of ca. 4 h subsequent to the UV/ TiO_2 treatment.

2 Experimental Section

2.1 Materials

All chemicals were used as received. The pesticide methyl-2-(dimethylamino)-*N*-{[(methyl- amino)carbonyl]oxy}-2-oxoethanimidothioate, referred to as Oxamyl, was supplied by Dr. Ehrenstorfer GmbH, Germany, in highly pure reagent grade form. The oral acute toxicity of Oxamyl LD_{50} (rat) is 2.5 mg kg^{-1} and LD_{50} (mouse) is 2.3 mg kg^{-1} ; additional information on the toxicity of Oxamyl is available elsewhere (Tomar 1997; European Food Safety Authority (EFSA) 2005). This pesticide is highly water-soluble ($\text{p}K = 6.2$), available for leaching and is relatively non-persistent in soil with its loss due mainly to decomposition via first-order kinetics degrading to <5% of the parent compound within 1 month of field application. Its reaction rate decreases with increase in concentration (Wagenet et al. 1984).

The pesticide methyl-*N*-{[(methylamino)carbonyl]oxy} ethanimidothioate, known commercially as Methomyl, was supplied by Wako Pure Chem. Co. Ltd. It has an oral acute toxicity of LD_{50} (rat) of 17 mg kg^{-1} and the LD_{50} (mouse) is 10 mg kg^{-1} (IPCS 1996). Methomyl is transformed in some greenhouse soils with half-lives of about 3–14 days. Microbial degradation appears to be the major transformation process in soil with CO_2 as the principal end product. However, a lag period of 1–2 weeks may be needed in unacclimatized soils before biodegradation begins. In aquatic ecosystems, hydrolysis half-lives of Methomyl in ethanol/water at pHs 6.0, 7.0, and 8.0 are 54, 38, and 20 weeks, respectively, at 25°C , whereas the hydrolysis half-life in pure water at 25°C is 37.5 weeks (MacCorquodale 2003).

The herbicide *N,N*-dimethyl- α -phenylbenzeneacetamide, also known as Diphenamid, was supplied by Kanto Chem. Co. Inc. It has an oral acute toxicity of $\text{LD}_{50} = 685 \text{ mg kg}^{-1}$ for the rat and 600 mg kg^{-1} for the mouse; for additional details, see also Ref. Cantavenera et al. 2006. The herbicide methyl-[(4-aminophenyl)sulfonyl]-carbamate, commercially named Asulam, was supplied by Wako Pure Chem. Co. Ltd. The latter has an oral acute toxicity LD_{50} (rat) that exceeds 5 g kg^{-1} and an acute inhalation LD_{50} (rat) that is greater than 5.0 mg kg^{-1} (Morales et al. 2002).

Titanium dioxide was Degussa P-25 with particle size 20–30 nm assessed by transmission electron microscopy; surface area $53 \text{ m}^2 \text{ g}^{-1}$ by BET methods; crystalline form 83% anatase and 17% rutile as determined by X-ray diffraction analysis.

2.2 Photomineralization Procedures

Aqueous solutions of each of the above substrates (0.10 mM; 50 mL; pH 4.5 unless noted otherwise) were placed in a 127-mL Pyrex vessel containing TiO₂ particles (100 mg; loading, 2.0 g L⁻¹) followed by supersonication to obtain uniform dispersions. The latter were subsequently purged with oxygen gas prior to UV irradiation. The TiO₂-containing aqueous dispersions were then illuminated with a 75-W mercury lamp (Toshiba SHL-100UVQ2) that emitted an irradiance of ca. 2.0 mW cm⁻² in the wavelength range 310–400 nm (maximal emission, 360 nm).

2.3 Analytical Procedures

The temporal evolution of CO₂ was assayed with a Shimadzu GC-8AIT gas chromatograph equipped with a TCD detector and a Porapack Q column; helium was the carrier gas. The loss of total organic carbon (TOC) in the dispersion was measured with a Shimadzu TOC-5000A TOC analyzer.

Additional measurements of the temporal degradation of Diphenamid (0.1 mM, 50 mL) were carried out in the presence of 100 mg of TiO₂ at pH 4.5. Opening of the rings during the photodecomposition of the Diphenamid and Asulam was monitored at 206 nm and 262 nm, respectively, with a JASCO V-570 UV–Visible spectrophotometer. The pH indicated in each of the Figures is the initial pH before UV illumination. When the pH of the degraded solution after a fixed time of illumination shifted gradually acidic, the surface charge of TiO₂ changes positively. The number of OH radicals which attack an organic substrate is the same as the number of protons formed theoretically.

Figure 2 illustrates the temporal spectral changes in the photodegradation of Diphenamid and Asulam. Formation of NH₄⁺ and NO₃⁻ ions was assayed on a

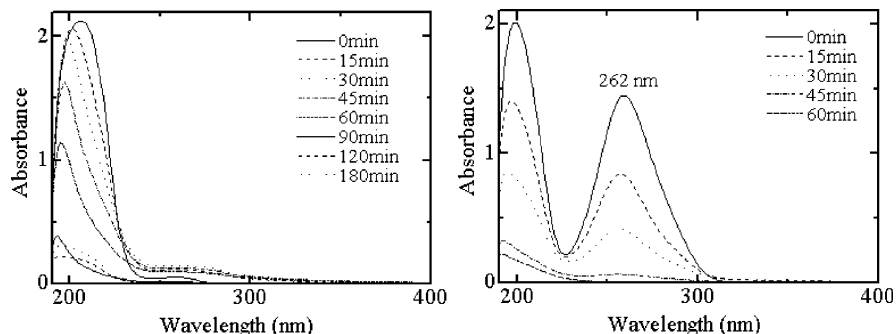


Fig. 2 Temporal spectral changes occurring during the photo-assisted degradation of (a) Diphenamid and (b) Asulam in aqueous TiO₂ dispersions

JASCO high-pressure liquid chromatographic system equipped with a CD-5 conductivity detector and either a Y-521 cationic column or an I-524 anionic column. Changes in the concentration of NH_4^+ ions were monitored with the JASCO ion chromatograph and the Y-521 cationic column; the eluent was nitric acid (4 mM). Nitrate ions were also monitored by ion chromatography with the I-524 anionic column using a mixed solution of phthalic acid (2.5 mM) and tris(hydroxymethyl) aminomethane (2.3 mM) as the eluent.

Fourier transform infrared spectroscopy (FT-IR; KBr method; JASCO spectrophotometer; Model FT/IR-620) was used in attempts to identify some of the intermediate products. Spectra were recorded after a freeze-dry procedure subsequent to removal of the TiO_2 particles from the photodegraded dispersions through filtration and/or centrifugation. Appropriate assignments of the observed IR bands were done according to standard infrared databases (Pouchert 1970; Schrader 1989; Socrates 2001).

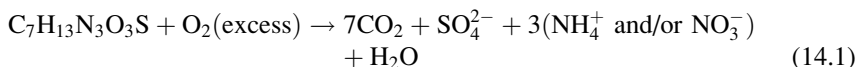
2.4 Point Charge and Electron Density Calculations (Dewar et al. 1985; Stewart 1989; Dewar and Yuan 1990; Horikoshi et al. 2003)

Molecular orbital calculations were performed by the parametric method 3 (PM3) with application of the Window MOPAC program. All the geometrical parameters for the above substances were calculated using the Broyden–Fletcher–Goldfarb–Shannon algorithm incorporated in the program for optimization, with the minimum energy obtained at the AM1 level. The geometries of the examined agrochemicals in aqueous solution were compared to those obtained in the gas phase by the conductor-like screening model orbital (COSMO) and electrostatic potential (point charge) calculations. The COSMO procedure generated a conducting polygonal surface around the system at van der Waal's distances. Standard values used herein were the number of geometrical segments per atom (NSPA) = 60; the dielectric constant was 78.4 at 25°C (in water). Initial positions of the OH radical attack are deduced from electron densities, whereas possible modes of closest approach of the agrochemical molecules onto the TiO_2 particle surface are inferred from the calculated point charges.

3 Results and Discussion

3.1 Photomineralization

The complete mineralization of Oxamyl, for example, as expressed by (14.1) should produce 35 μmols of carbon dioxide for an initial concentration of 5 μmols in the 50-mL dispersion (0.1 mM)



The temporal evolution of CO₂ gas (in % yield) produced in the photo-assisted degradation of the two pesticides and herbicides and monitored by gas chromatography is shown in Fig. 3. In all the cases, formation of carbon dioxide increased with increasing irradiation time attaining approximately 90% mineralization after ca. 4 h of UV illumination.

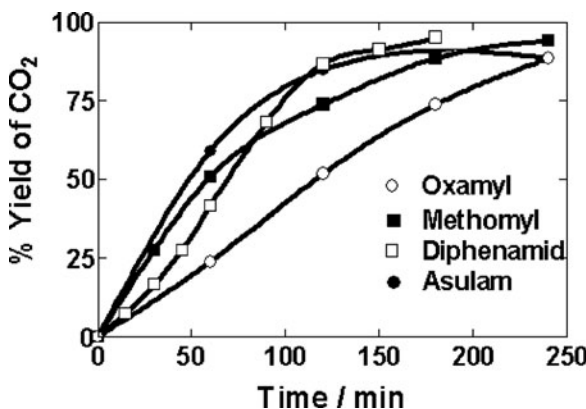


Fig. 3 Temporal CO₂ evolution yield (%) in the photo-assisted mineralization of Oxamyl, Methomyl, Diphenamid, and Asulam; initial concentrations of each, 0.10 mM in 50-mL dispersions (pH 4.5)

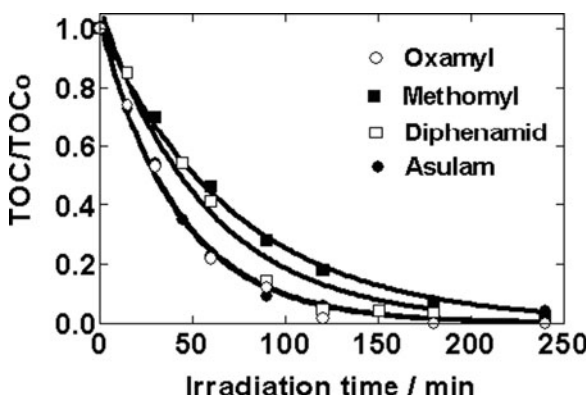


Fig. 4 Normalized temporal decrease of TOC in the photo-assisted degradation of Oxamyl, Methomyl, Diphenamid, and Asulam (pH 4.5). Initial concentrations in carbon content were, respectively, 6.6 ppm, 4.1 ppm, 19.1 ppm, and 9.2 ppm

The comparatively temporal decrease of TOC in the degradation of the two pesticides and the two herbicides is depicted in Fig. 14.4. TOC loss for Oxamyl organic carbon is 100% complete within 4 h into the mineralization process. In all the other cases, TOC loss is also quantitative and followed first-order kinetics with the rates being Diphenamid (19.5 ppm h^{-1}) > Asulam (12.7 ppm h^{-1}) > Oxamyl (9.1 ppm h^{-1}) > Methomyl (3.4 ppm h^{-1}), in reasonable accord with the trend in CO_2 evolution. Note that the slight discrepancies between the extent of CO_2 evolution (Fig. 3) and loss of TOC (Fig. 4) are due to the forms of CO_2 present at the prevailing pH of 4.5 ($\text{CO}_2 \cdot \text{H}_2\text{O} \approx \text{H}_2\text{CO}_3 \approx \text{H}^+ + \text{HCO}_3^-$; $pK_{\text{a}1} = 6.4$) in the form of small quantities of bicarbonate species during the chromatographic determinations of CO_2 .

3.2 Conversion of N and S Functions

The temporal formation of NH_4^+ , NO_3^- , and SO_4^{2-} ions against UV irradiation time in the photo-assisted mineralization of Oxamyl is shown in Fig. 5. Under acidic conditions (pHs 3.0 and 4.5), the generated amount of NH_4^+ ions was significantly greater than that of NO_3^- ions, which typically showed a lag time before its formation. By contrast, the amount of generated SO_4^{2-} ions was far smaller than expected, particularly at pH 3.0. We suppose that since the surface of TiO_2 catalyst is positively charged, the doubly charged SO_4^{2-} anions may remain adsorbed on the TiO_2 surface, thereby mitigating somewhat the quantity of SO_4^{2-} ion detected in the aqueous bulk solution. By comparison, at pH 4.5 the observed quantity of SO_4^{2-} ions increased while the amount of NH_4^+ ions formed decreased, whereas the amount of NO_3^- ions produced remained nearly constant at both acidic pHs. On the other hand, the quantity of NO_3^- anions formed at the alkaline pH of 11.0 was more significant than the quantity of NH_4^+ ions produced. As well, the amount of sulfate anions produced was more significant the more alkaline the solution bulk becomes, since adsorption is no longer a restrictive factor owing to electrostatic repulsion between the negatively charged TiO_2 surface and the sulfate anions. However, we also cannot preclude that the smaller quantity of ammonium ions observed in alkaline media may be due to a certain quantity of NH_4^+ that is oxidized to NO_3^- ions (Pollema et al. 1992). The stoichiometric sum of both NH_4^+ and NO_3^- ions produced in the photomineralization of Oxamyl (initial concentration, 0.1 mM) bearing three nitrogen atoms should theoretically be 0.30 mM. Experimentally we find the combined total amount of NH_4^+ and NO_3^- ions at pH 3.0 to be 0.297 mM after 4 h of UV illumination of the aqueous TiO_2 dispersion indicating maximal conversion of the N functions within experimental error. At pH 4.5, the $[\text{NH}_4^+ + \text{NO}_3^-]$ sum was 0.28 mM after the 4-h illumination period, whereas in alkaline media (pH 11.0), the sum was ~ 0.24 mM corresponding to about 80% of the expected amount.

The temporal formation of SO_4^{2-} , NH_4^+ , and NO_3^- ions during the photodegradation of Methomyl at pHs 3.0, 7.0, and 11.0 is illustrated in Fig. 6. The same

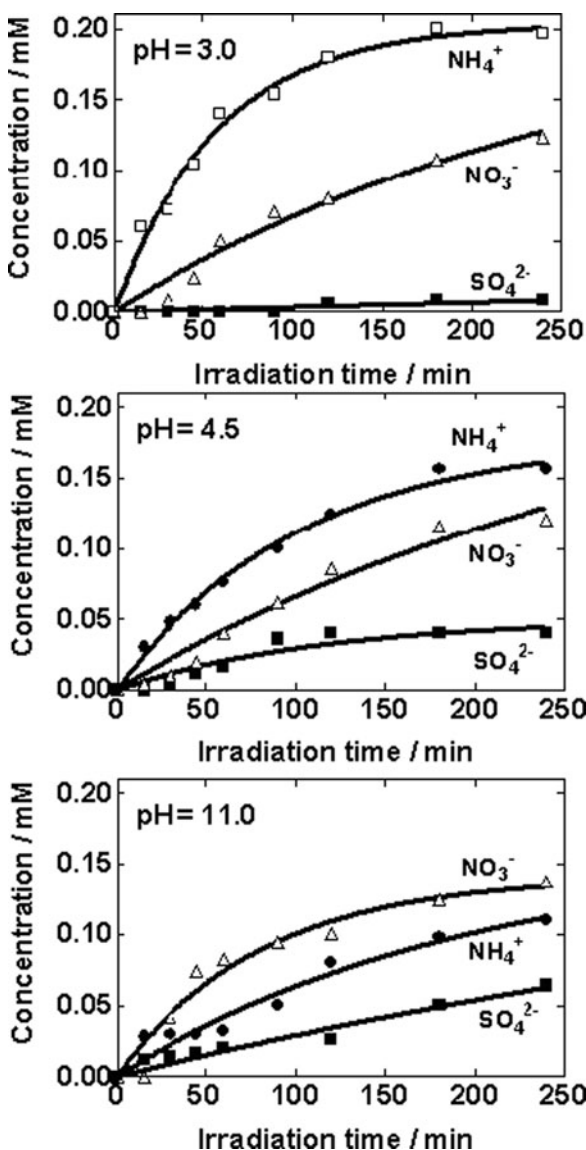


Fig. 5 Formation of SO_4^{2-} , NH_4^+ , and NO_3^- ions in the photodegradation of Oxamyl (initial concentration, 0.1 mM in 50 mL) at pHs 3.0, 4.5, and 11.0

tendency is evident with respect to Methomyl as observed in the case of Oxamyl. That is, the amount of SO_4^{2-} anions produced at pH 3.0 was relatively small owing to electrostatic attraction on the positive TiO_2 surface. By contrast, at pH 11.0 the amount of sulfate anions produced was greater attributable to repulsion between the negatively charged TiO_2 surface and SO_4^{2-} anions. Contrary to Oxamyl, however,

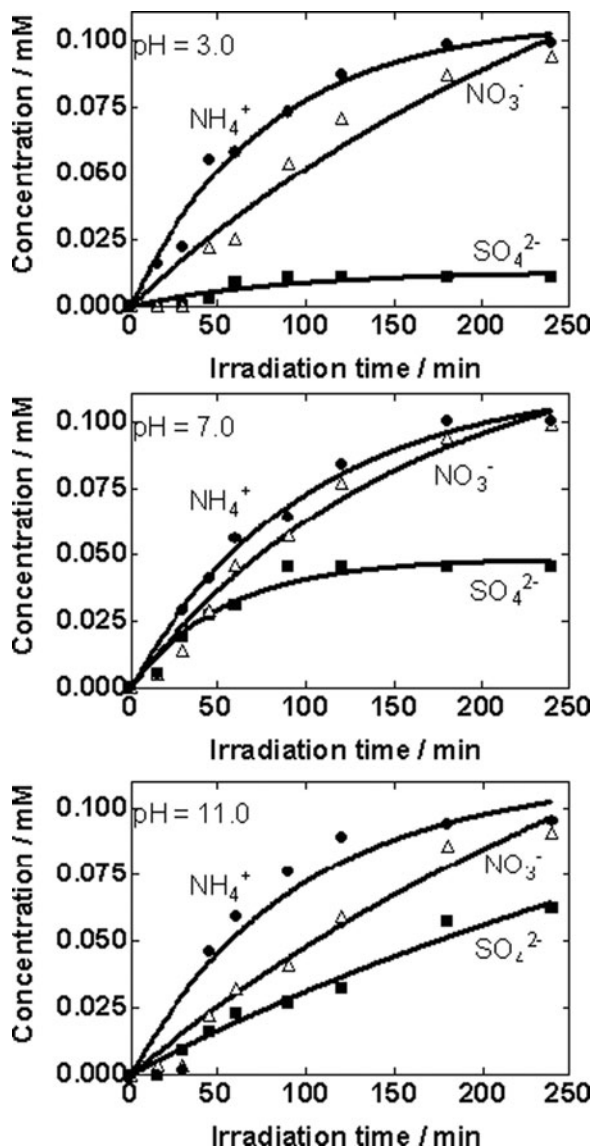


Fig. 6 Formation of SO_4^{2-} , NH_4^+ , and NO_3^- ions in the photodegradation of Methomyl (0.1 mM, 50 mL) at pHs 3.0, 7.0, and 11.0

the quantity of NH_4^+ cations formed during the degradation of Methomyl was always greater than the quantity of NO_3^- ions produced even under alkaline conditions of pH 11.0. The total amount of NH_4^+ and NO_3^- ions formed and expected to be theoretically 0.20 mM for the mineralization of Methomyl (0.1 mM) after 240 min of UV illumination reached 0.19 mM at pH 3.0, 0.20 at pH 7.0, and 0.19 mM at pH 11.0.

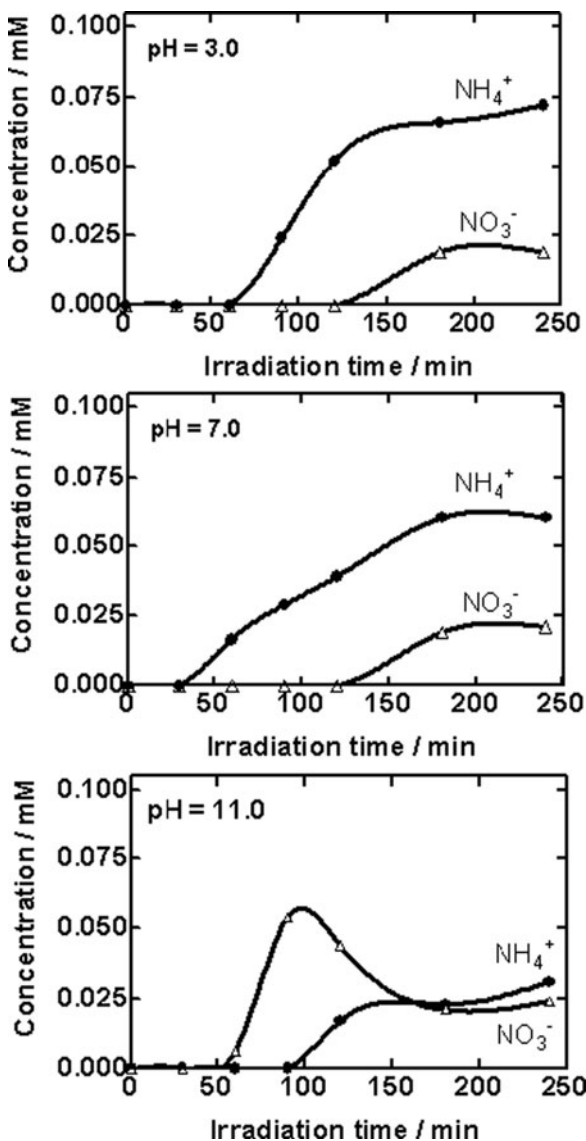


Fig. 7 Formation of NH_4^+ and NO_3^- anions during the photo-assisted degradation of Diphenamid (0.1 mM, 50 mL) at pHs 3.0, 7.0, and 11.0

The temporal evolution of ammonium and nitrate ions produced during the photo-assisted transformation of the nitrogen functions at pHs 3.0 and 7.0 in the Diphenamid structure is depicted in Fig. 7. After ca. 4 h into the process, approximately 19% of the nitrogen was converted into NO_3^- ions and ca. 72% into NH_4^+

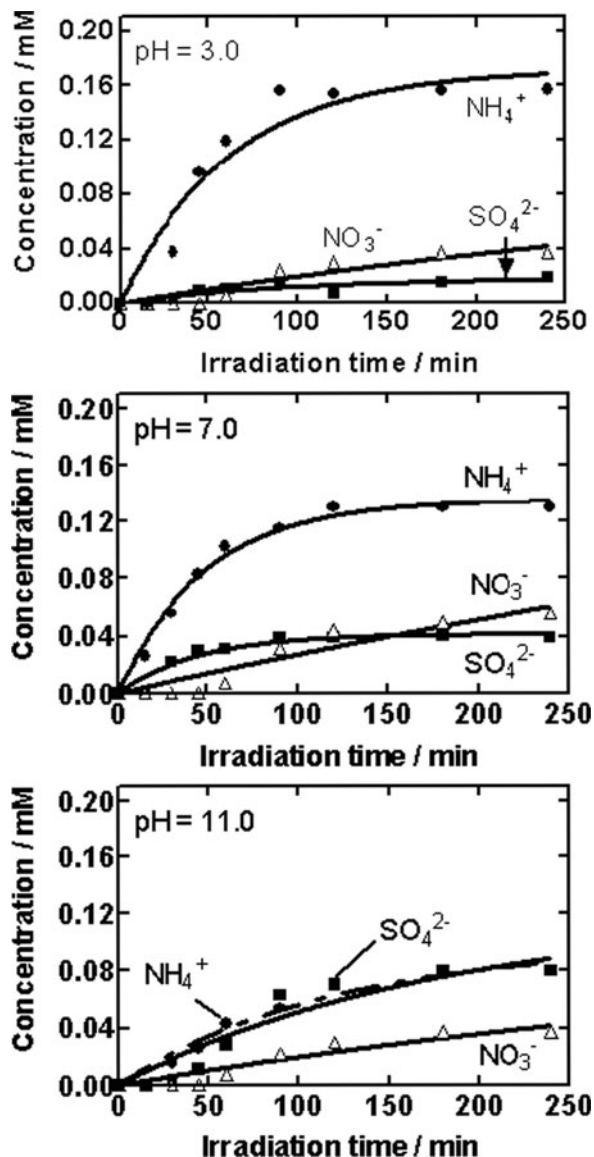


Fig. 8 Formation of SO_4^{2-} , NH_4^+ , and NO_3^- ions in the photo-assisted degradation of Asulam (0.1 mM, 50 mL) at pHs 3.0, 7.0, and 11.0

ions, giving a total of 91% at pH 3.0 or about 0.091 mM against a theoretical estimate of 0.10 mM. At pH 7.0, approximately 21% of the N function was transformed into NO_3^- ions and ca. 60% into NH_4^+ ions for a total of 81% or

0.081 mM. The remaining nitrogen was probably converted to primary and/or secondary amines, although they were not identified. At pH 11.0, both NH_4^+ and NO_3^- ions were also produced under such alkaline aqueous conditions.

Formation of SO_4^{2-} , NH_4^+ , and NO_3^- ions in the photodegradation of Asulam at pHs 3.0, 7.0, and 11.0 is depicted in Fig. 8.

Examining the pH dependence of the degradation of Asulam after 4 h into the process, the amount of NH_4^+ ions formed decreased in the order: pH 3.0 (0.16 mM) > pH 7.0 (0.13 mM) > pH 11.0 (0.080 mM). By contrast, the quantity of NO_3^- ions produced varied in the order: pH 3.0 (0.037 mM) > pH 7.0 (0.054 mM) < pH 11.0 (0.037 mM). The total sum of both NH_4^+ and NO_3^- ions produced was: pH 3.0 (0.19 mM) \geq pH 7.0 (0.18 mM) > pH 11.0 (0.12 mM), against the expected 0.20 mM. With respect to the quantity of SO_4^{2-} anions generated, a larger amount was produced in alkaline media (pH 11.0; 0.080 mM) than in neutral (pH 7.0; 0.039 mM) or acidic media (pH 3.0; 0.019 mM). Again it is tempting to attribute the greater quantity in alkaline media to electrostatic desorption (or repulsion) of SO_4^{2-} anions from the negatively charged TiO_2 surface at pH 11.0 than is the case in acidic media where the particle surface is positively charged.

Table 1 summarizes the dynamics of the photomineralization of the four substrates in terms of rates of evolution of carbon dioxide and conversion of the N and S functions into NH_4^+ and NO_3^- , and SO_4^{2-} anions, respectively, at three different pHs. The rates of formation of CO_2 varied in the order: Diphenamid > Asulam > Methomyl \geq Oxamyl, indicating that mineralization of the herbicides possessing an aromatic-ring is faster than for the non-aromatic pesticides. Formation of nitrate ions often necessitated a lag time before its formation could be detected, and was particularly significant in the degradation of Diphenamid and Asulam. Regardless, conversion of the N and S functions followed the first-order kinetics. A glance at the first-order rates shows that reduction of the N function predominates in acidic media, at least for Oxamyl, Diphenamid, and Asulam contrary to Methomyl for which NH_4^+ ion formation appears to be faster in alkaline media. By contrast, oxidation of N to give nitrate ions tends to predominate in alkaline media. Transformation of the S function appears best carried out at near neutral conditions according to the dynamics displayed in Table 1.

3.3 Identification of Some Intermediates by FTIR

The temporal changes observed in the infrared (FTIR) spectral patterns in the 400–1,800 cm^{-1} wavenumber region for the degraded products of Oxamyl are illustrated in Fig. 9.

The IR spectrum of Oxamyl has two strong characteristic bands at 1,736 cm^{-1} , one of which is attributable to the ketone C=O stretching vibration and the other at 1,716 cm^{-1} is assigned to the ester $-\text{O}-\text{C}=\text{O}$ carbonyl stretching mode. This initial absorption peak of the ester at 1,716 cm^{-1} disappeared after 1 h of UV illumination,

Table 1 Summary of the dynamics of CO_2 evolution and formation of NH_4^+ , NO_3^- , and SO_4^{2-} ions during the photo-assisted degradation of the substrates examined

Kinetics	Oxamyl	R or k		Methomyl		Diphenamid		Asulam				
		Lag (min)	pH	Lag (min)	k	pH	Lag (min)	k	pH	Lag (min)	k	pH
R_{CO_2} ($\mu\text{mol h}^{-1}$)	—	14.3	4.5	—	17.3	4.5	—	54.7	4.5	—	35.0	4.5
$k_{\text{NH}_4^+}$ (h^{-1})	0	1.03	3.0	0	0.78	3.0	60	0.96	3.0	15	0.96	3.0
	0	0.58	4.5	0	0.60	7.0	30	0.51	7.0	0	1.20	7.0
	0	0.30	11.0	15	1.14	11.0	90	—	11.0	15	0.50	11.0
$k_{\text{NO}_3^-}$ (h^{-1})	15	0.22	3.0	30	0.20	3.0	120	1.26	3.0	45	0.12	3.0
	0	0.19	4.5	0	0.38	7.0	120	1.26	7.0	45	0.060	7.0
	15	0.74	11.0	0	0.41	11.0	30	—	11.0	45	0.11	11.0
$k_{\text{SO}_4^{2-}}$ (h^{-1})	90	0.0078	3.0	30	0.67	3.0	—	—	15	15	0.66	3.0
	15	0.51	4.5	0	1.09	7.0	—	—	—	15	1.32	7.0
	0	0.092	11.0	15	0.37	11.0	—	—	15	15	0.33	11.0

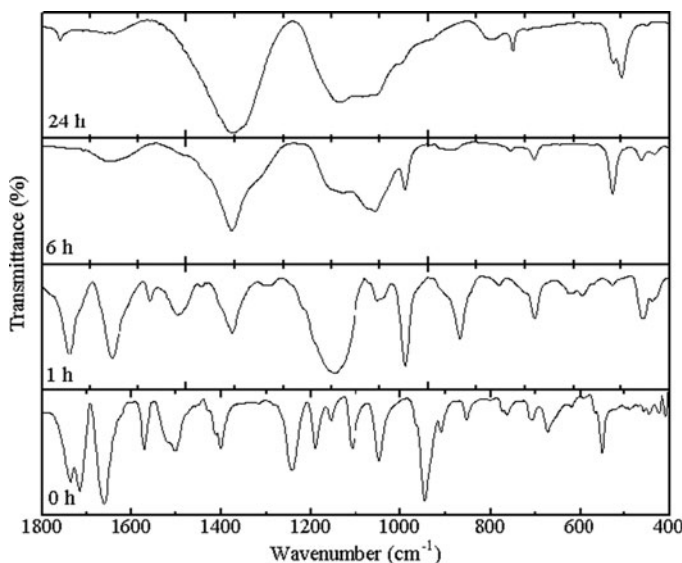


Fig. 9 Temporal variations in the FT-IR spectral patterns during the photodegradative process for Oxamyl spanning a 24-h period. Initial concentration was 1.0 mM and thus required longer irradiation times for the degradation

whereas the ketone carbonyl signal still remained strong. It would appear therefore that the ester group in Oxamyl can be cleaved more easily than the ketone carbonyl. The secondary $-\text{NH}-\text{CH}_3$ and tertiary $-\text{N}=(\text{CH}_3)_2$ amines in Oxamyl have a strong intensity band in the neighborhood of $3,300 \text{ cm}^{-1}$ (not shown) that is attributable to N–H stretching vibrations. After UV illumination for more than 1 h, this broad band broadened even more and spanned the range $3,000$ – $3,500 \text{ cm}^{-1}$, which suggests an increase in the extent of O–H group stretching vibrations in the photooxidation of Oxamyl. Although the $\text{S}-\text{CH}_3$ group in Oxamyl can be mineralized to SO_4^{2-} ions, the intermediate product $\text{CH}_3\text{SO}_3\text{H}$ was also identified by IR spectroscopy. A strong absorption band at $1,662 \text{ cm}^{-1}$ was observed after 1 h of irradiation and is attributed to the tertiary amide group in Oxamyl. The peak intensity of the $1,667 \text{ cm}^{-1}$ band showed a remarkable decrease.

The strong broad band at $1,405 \text{ cm}^{-1}$ still present even after the 24-h irradiation period is assigned to the $-\text{N}<(\text{CH}_3)_2$ group, indicating the presence of some dimethylamine derivative.

3.4 Point Charges and Electron Densities

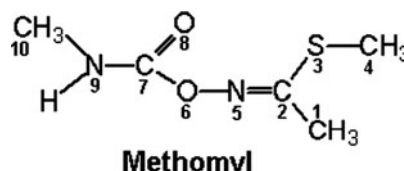
The calculated point charges and electron densities for all non-hydrogen atoms in both the gas phase and in the presence of water molecules for Oxamyl, Methomyl, Diphenamid, and Asulam are reported in Tables 2–5, respectively.

Table 2 Molecular orbital calculation of electron densities and point charges for Oxamyl

Atom no	Type	Point charge		Electron density	
		Gas	Water	Gas	Water
1	C	0.3455	0.3754	3.6545	3.6246
2	O	-0.3449	-0.5227	6.3449	6.5227
3	N	-0.3178	-0.2616	5.3178	5.2616
4	C	-0.0829	-0.1051	4.0829	4.1051
5	C	-0.0799	-0.1123	4.0799	4.1123
6	C	-0.2476	-0.2281	4.2476	4.2281
7	S	0.2931	0.2366	5.7069	5.7634
8	C	-0.3877	-0.3856	4.3877	4.3855
9	N	-0.0472	-0.0582	5.0473	5.0582
10	O	-0.1882	-0.2237	6.1882	6.223
11	C	0.4089	0.4780	3.5911	3.522
12	O	-0.3325	-0.5454	6.3325	6.5454
13	N	-0.3647	-0.3107	5.3647	5.3106
14	C	-0.0728	-0.0961	4.0727	4.0961

As noted earlier, the atoms that approach most closely the positively charged TiO_2 particle surface will be those with the greatest negative point charge, which in the case of Oxamyl are the O^2 and O^{12} carbonyl oxygens; for Methomyl the largest negative point charge rests on the O^8 carbonyl oxygen, whereas for Diphenamid it lies on the O^3 carbonyl oxygen. By contrast, in the Asumal structure the largest negative point charge lies on the two sulfonyl oxygens O^9 and O^{10} followed by the phenyl C^4 carbon. What is also notable in these calculated point charges is that the negative charge on the atoms noted above is remarkably made more negative in water than they are in the gas phase. Accordingly, these will be the atoms that approach the particle surface in acidic media when the surface is positively charged. In alkaline media where the particle surface is negatively charged, the atoms that will approach most closely the surface are expected to be the corresponding carbonyl carbons in Oxamyl, Methomyl and Diphenamid, and the sulfonyl sulfur in the case of Asumal all of which bear the largest positive point charge.

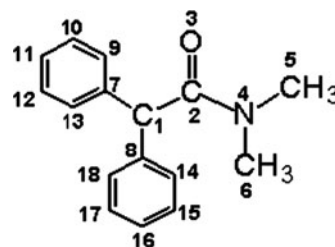
More important, however, in TiO_2 photo-assisted oxidations will be the positions with the greatest electron density that will be most significant, as these sites are the ones most likely to be the points of attack by the photogenerated OH radicals. Evidently from Tables 2–5, these sites would appear to be the same

Table 3 Molecular orbital calculation of electron densities and point charges for Methomyl

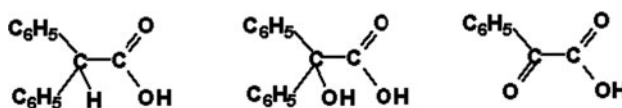
Atom no	Type	Point charge		Electron density	
		Gas	Water	Gas	Water
1	C	-0.1723	-0.2169	4.1723	4.2169
2	C	-0.1935	-0.1277	4.1935	4.1277
3	S	0.2172	0.2237	5.7828	5.7763
4	C	-0.3645	-0.3954	4.3645	4.3954
5	N	-0.0899	-0.1685	5.0899	5.1684
6	O	-0.2099	-0.2446	6.2099	6.2446
7	C	0.4130	0.4284	3.5870	3.5716
8	O	-0.3493	-0.5374	6.3493	6.5374
9	N	-0.3655	-0.3021	5.3655	5.3020
10	C	-0.0711	-0.1053	4.0711	4.1053

oxygen atoms that bore the largest negative point charges. However, it is more likely that the sites for ·OH radical attack be the atoms adjacent to these oxygens, namely the N⁵, N⁹, and N¹³ nitrogens, and the sulfur atom S⁷ in Oxamyl, in the latter case yielding methylsulfonic acid as an intermediate and ultimately SO₄²⁻ ions. In Methomyl they are the nitrogens N⁵ and N⁹ as well as the S³ sulfur atom again producing CH₃SO₃H and ultimately sulfate anions. Attack on the nitrogens begins the path toward formation of nitrate and ammonium ions through what would be, no doubt, a complex mechanism.

In the herbicide Diphenamid, the most probable position of ·OH radical attack should be the N⁴ atom to yield a dimethylhydroxyl amine and diphenylacetic acid as the first two possible intermediates toward mineralization. Note that we made no attempt in this study to identify the intermediates photogenerated during the mineralization process as this was not the present goal. The work of Rahman and coworkers (2003) on the photodegradation of Diphenamid identified no less than five intermediates (**I–V**) under conditions that were not very dissimilar from the ones used herein. Formation of these byproducts was suggested to take place by attachment of an ·OH radical at the carbonyl C² with loss of methylamine yielding species **I**, followed by further attack by the reactive oxygen species ·OH and/or ·OOH radicals producing intermediate **II**, and subsequent loss of benzene giving species **III**. By contrast, intermediate **IV** was derived from an oxidative process involving electron transfer to either the ·OH and/or ·OOH radicals or to the valence band holes (that is, direct hole oxidation), whereas species **V** was formed by ·OH radical abstraction of the α-hydrogen at the C¹ position in the Diphenamid structure (see Table 4).

Table 4 Molecular orbital calculation of electron densities and point charges for Diphenamid

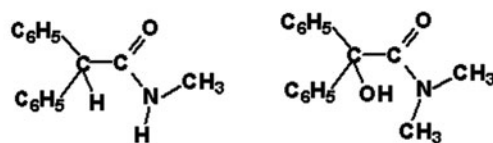
Atom no	Type	Point charge		Electron density	
		Gas	Water	Gas	Water
1	C	-0.9641	-0.08260	4.0015	4.0055
2	C	0.6436	0.6793	3.7365	3.6681
3	O	-0.3582	-0.5573	6.3562	6.5593
4	N	-0.2842	-0.2237	5.0692	5.0246
5	C	-0.2233	-0.2604	4.0750	4.0930
6	C	-0.0688	-0.0775	4.0872	4.1094
7	C	0.4962	0.3229	4.0823	4.0956
8	C	0.3222	0.2517	4.0765	4.1024
9	C	-0.3265	-0.2756	4.1019	4.1166
10	C	-0.1285	-0.2009	4.1028	4.1277
11	C	-0.1851	-0.1695	4.0974	4.1222
12	C	-0.0888	-0.1896	4.0977	4.1277
13	C	-0.3912	-0.3078	4.0890	4.1294
14	C	-0.2673	-0.3256	4.0856	4.1251
15	C	-0.1446	-0.1318	4.0995	4.1234
16	C	-0.1401	-0.2034	4.0972	4.1196
17	C	-0.1737	-0.1817	4.1043	4.1265
18	C	-0.2229	-0.1985	4.0959	4.1103



I

II

III



IV

V

Table 5 Molecular orbital calculations of electron densities and point charges for Asulam

Atom no	Type	Point charge		Electron density	
		Gas	Water	Gas	Water
1	C	0.1771	0.2204	3.8229	3.7796
2	C	-0.2449	-0.2984	4.2450	4.2984
3	C	0.0406	0.0186	3.9594	3.9814
4	C	-0.9341	-1.0274	4.9341	5.0274
5	C	0.0406	0.0664	3.9594	3.9336
6	C	-0.2449	-0.3276	4.2450	4.3276
7	N	-0.3666	-0.3130	5.3666	5.3130
8	S	2.887	3.0271	3.1128	2.9729
9	O	-0.9193	-1.0875	6.9193	7.0875
10	O	-0.9194	-1.0842	6.9194	7.0842
11	N	-0.8245	-0.7958	5.8245	5.7958
12	C	0.4141	0.5122	3.5859	3.4878
13	O	-0.3635	-0.5279	6.3635	6.5279
14	O	-0.2796	-0.2905	6.2796	6.2905
15	C	-0.0534	-0.0699	4.0534	4.0699

Asulam possesses two pK_a s of 1.3 and 4.1 (Catastini et al. 2002b) so that at pH 3.0 it exists in its neutral form, whereas at pH 7.0 it exists in its deprotonated form at the N¹¹ position, thereby increasing the electronic density at this N atom. In the same reasoning as above then, in the case of Asulam, ·OH radical attack should occur at N¹¹ and at the phenyl C⁴ positions to give a sulfonic acid and an aminophenol. The intermediates identified by Catastini and coworkers (1992b) were the parasulfanilic acid and benzoquinone with traces of hydroquinone. The latter two were likely the result of photooxidation of the aminophenol known to degrade fairly rapidly under conditions somewhat similar to those used here (Serpone et al. 1998).

4 Concluding Remarks

This study examined the quantitative TiO₂ photo-assisted mineralization of two widely used pesticides and herbicides as evidenced by the evolution of carbon dioxide and by the loss of total organic carbon in aqueous dispersions under acidic

(pH 3.0), neutral (pH 7.0), and alkaline (pH 11.0) conditions. Conversion of the N functions into ammonium ions (or ammonia) appears to predominate at pH ≤ 7 , whereas formation of nitrate ions seems dominant in alkaline media. Nonetheless, the conversion is also nearly quantitative. The S function is transformed into SO_4^{2-} ions, the quantity of which increased toward more alkaline conditions.

Acknowledgments Our work in Tokyo is sponsored by the Ministry of Education, Culture, Sports, Science and Technology of Japan (Grand-in-Aid for Scientific Research (c) No. 17550145 to H.H.), whereas the research in Pavia has been supported by a grant from the Ministero dell'Istruzione, dell'Università e della Ricerca (MIUR-Roma; to N.S.). We are grateful to Ms. T. Ohno (Josai University) for the molecular orbital simulation as well as to Miss M. Itou, Miss R. Terayama, and Dr. T. Koike (Meisei University) for technical assistance.

References

- Bank S, Tyrrell RJ (1984) Kinetics and mechanism of alkaline and acidic hydrolysis of aldicarb. *J Agric Food Chem* 32:1223–1232
- Bromilow RH, Briggs GG, Williams MR, Smelt JH, Tuinstra LGMT, Traag WA (1986) The role of ferrous ions in the rapid degradation of oxamyl, methomyl and aldicarb in anaerobic soils. *Pestic Sci* 17:535–547
- Bruff SA, Griffin JL, Richard EP (1995) Influence of rainfree period after asulam application on johnsongrass (*Sorghum halepense*) control. *Weed Technol* 9:316–320
- Cantavenera MJ, Catanzaro I, Loddo V, Palmisano L, Sciandrello G (2007) Photocatalytic degradation of paraquat and genotoxicity of its intermediate products. *J Photochem Photobiol A: Chem*, 185: 277–282
- Catastini C, Sarakha M, Mailhot G (2002a) Asulam in aqueous solutions: fate and removal under solar irradiation. *Int J Environ Anal Chem* 82:591–600
- Catastini C, Mailhot G, Malato S, Sarakha M (2002b) Iron (III) aqua-complexes as catalysts for pesticides mineralisation by sunlight irradiation. Proceedings workshop 2002, Plataforma Solar de Almeria, Spain
- Chapman RA, Cole CM (1982) Observations on the influence of water and soil pH on the persistence of insecticides. *J Environ Sci Health B* 17:487–504
- Cohen ZZ, Eiden C, Lober MN (1986) Evaluation of pesticide in ground water. In: Gerner WY (ed) American Chemical Society, Washington, D.C., ACS Symp. Ser. 315, 170–196
- Cox L, Hermosyn MC, Cornejo J (1993) Adsorption of methomyl by soils of Southern Spain and soil components. *Chemosphere* 27:837–849
- Defelice M (1999) Introduction and history of cell division inhibitor herbicides. *Crops insights*. Pioneer Hi-Bred International Inc. 9, No. 15
- Dewar MJS, Zoebisch EG, Healy EF, Stewart JJP (1985) Development and use of quantum mechanical molecular models. 76. AM1: a new general purpose quantum mechanical molecular model. *J Am Chem Soc* 107:3902–3909
- Dewar MJS, Yuan Y-C (1990) AM1 parameters for sulfur. *Inorg Chem* 29:3881–3890
- Dowd RM, Anderson MP, Johnson MI (1988) Ground water monitoring geophysical methods. In: Proceedings of the 2nd National Outdoor Action Conference on aquifer restoration. National Water Well Association, Dublin, OH, pp 1365–1379
- Elmore CL, Humphrey WA, Kretchum T (1968) Preemergence weed control in ground cover plantings. *California Turfgrass Cult* 18:9–10

- European Food Safety Authority (EFSA) (2005) Conclusion regarding the peer review of the pesticide risk assessment of the active substance oxamyl. EFSA Sci Rep 26:1–78
- Food and Agriculture Organization of the United Nations (FAO) and the World Health Organization (WHO) (1985) Pesticide residues in food – 1983. Data and recommendations of the joint meeting of the FAO Panel of Experts on Pesticide Residues in Food and the Environment and the WHO Expert Group on Pesticide Residues, Geneva, 5–14 December 1983; <http://www.inchem.org/documents/jmpr/jmpmono/v83pr33.htm>
- Garthwaite DG, Thomas MR, Anderson H, Stoddart H (2005) Pesticide usage survey report 202 Arable Crops in Great Britain 2004. Department for Environment, Food and Rural Affairs and the Scottish Executive Environment and Rural Affairs Dept. Central Science Laboratory, York, UK; see also, <http://www.csl.gov.uk/science/organ/pvm/puskm/arable2004.pdf>
- Gerstl Z (1984) Adsorption, decomposition and movement of oxamyl in soil. Pestic Sci 15:9–17
- Gianessi LP, Marcelli MB (2000) Pesticide use in U.S. Crop production: 1997. National summary report. National Center for Food and Agricultural Policy, Washington, DC
- Graebing P, Frank MP, Chib JS (2003) Soil photolysis of herbicides in a moisture- and temperature-controlled environment. J Agric Food Chem 51:4331–4337
- Harvey J, Han JCY (1978) Decomposition of oxamyl in soil and water. J Agric Food Chem 26:536–541
- Hassall KA (1990) The biochemistry and uses of pesticides, 2nd edn. VCH, New York
- Hegarty AF, Frost LN (1973) Elimination-addition mechanism for the hydrolysis of carbamates. Trapping of an isocyanate intermediate by an o-amino-group. J Chem Soc Perkin Trans 2:1719–1728
- Hidaka H, Nohara K, Zhao J, Serpone N, Pelizzetti E (1992a) Photo-oxidative degradation of the pesticide permethrin catalysed by irradiated TiO₂ semiconductor slurries in aqueous media. J Photochem Photobiol A: Chem 64:247–257
- Hidaka H, Jou H, Nohara K, Zhao J (1992b) Photocatalytic degradation of the hydrophobic pesticide permethrin in fluoro surfactant/TiO₂ aqueous dispersions. Chemosphere 25:1589–1598
- Horikoshi S, Hidaka H, Serpone N (2003) Environmental remediation by an integrated microwave/UV-illumination technique: IV. Non-thermal effects in the microwave-assisted degradation of 2, 4-dichlorophenoxyacetic acid in UV-irradiated TiO₂/H₂O dispersions. J Photochem Photobiol A: Chem 159:289–300
- Hornsby AG, Wauchope RD, Herner AE (1996) Pesticide properties in the environment. Springer, New York
- Ishiki RR, Ishiki HM, Takashima K (2005) Photocatalytic degradation of Imazetha-pyr herbicide at TiO₂/H₂O interface. Chemosphere 58:1461–1469
- Kolpin DW, Barbash JE, Gilliom RJ (2000) Pesticides in ground water of the United States, 1992–1996. Ground Water 38:858–863
- MacCorquodale DS (2003) Chemical fact sheet: methomyl. Spectrum Laboratories Inc. Georgia; <http://www.speclab.com/compound/c1675277.htm>
- Malato S, Blanco J, Richter C, Fernandez P, Maldonado MI (2000) Solar photocatalytic mineralization of commercial pesticides: oxamyl. Sol Energy Mater Sol Cells 64:1–14
- Marrs RH, Frost AJ, Plant RA, Lunnis P (1992) Aerial applications of asulam: a bioassay technique for assessing buffer zones to protect sensitive sites in upland Britain. Biol Conserv 59:19–23
- Morales JJ, Liccione J, O'Keef B (2002) Asulam. HED human health assessment for the Tolerance Reassessment Eligibility Decision (TRED). Chemical No. 106901/02. No MRID #. DP Barcode No. D276505. Office of Prevention, Pesticides and Toxic Substances, United States Environmental Protection Agency (EPA); http://www.epa.gov/oppssrd1/REDs/asulam_tred.pdf
- Moye HA, Miles CJ (1988) Aldicarb contamination of groundwater. Rev Environ Contam Toxicol 105:99–146

- Muszkat I, Raucher D, Magaritz M, Romen D (1994) Groundwater contamination by organic pollutants. In: Zoller U (ed) *Ground water contamination and control*. Marcel Dekker, New York, pp 257–271
- Muszkat L, Bir L, Feigelson L (1995) Solar photocatalytic mineralization of pesticides in polluted waters. *J Photochem Photobiol A: Chem* 87:85–88
- Parsons S (2004) Advanced oxidation processes for water and wastewater treatment. IWA Publishing Ltd, London
- Pelizzetti E, Mauriono V, Minero C, Carlin V, Pramauro E, Zerbinati O, Tosato ML (1990) Photocatalytic degradation of atrazine and other s-triazine herbicides. *Environ Sci Technol* 24:1559–1565
- Pelizzetti E, Minero C, Piccinini P, Vincenti M (2003) Phototransformations of nitrogen containing organic compounds over irradiated semiconductor metal oxides: nitrobenzene and atrazine over TiO₂ and ZnO. *Coord Chem Rev* 125:183–193
- Pollema CH, Milosavljević EB, Hendrix JL, Solurić L, Nelson JH (1992) Photocatalytic oxidation of aqueous ammonia (ammonium ion) to nitrite or nitrate at titanium dioxide particles. *Monatsh Chem* 123:333–339
- Pouchert CJ (1970) The aldrich library of infrared spectra. The Aldrich Chemical Co. Inc
- Rahman MA, Muneer M, Bahnamann D (2003) Photocatalyzed degradation of a herbicide derivative, diphenamid in aqueous suspension of titanium dioxide. *J Adv Oxid Technol* 6:100–108
- Schrader B (1989) Raman/infrared atlas of organic compounds, 2nd edn. VCH Publishers, New York
- Serpone N, Calza P, Salinaro A, Cai L, Emeline A, Hidaka H, Horikoshi S, Pelizzetti E (1998) What becomes of nitrogen in the photoelectrochemical and photocatalyzed mineralization of N-containing substances at titania/water interfaces? Proceedings of the conference of the electrochemical society. 97-20, pp 301–320
- Smelt JH, Dekker A, Leistra M, Houw NWH (1983) Conversion of four carbamoyloximes in soil samples from above and below the soil water table. *Pestic Sci* 14:173–181
- Socrates G (2001) Infrared and Raman characteristic group frequencies, 3rd edn. Wiley, New York
- Stewart JJP (1989) Optimization of parameters for semiempirical methods. I. Method *J Comp Chem* 10:209–220
- Strathmann TJ, Stone AT (2001) Reduction of the carbamate pesticides oxamyl and methomyl by dissolved Fe^{II} and Cu^I. *Environ Sci Technol* 35:2461–2469
- Strathmann TJ, Stone AT (2002a) Reduction of the pesticides oxamyl and methomyl by Fe^{II}: effect of pH and inorganic ligands. *Environ Sci Technol* 36:653–661
- Strathmann TJ, Stone AT (2002b) Reduction of oxamyl and related pesticides by Fe^{II}: influence of organic ligands and natural organic matter. *Environ Sci Technol* 36:5172–5183
- The International Programme on Chemical Safety (IPCS) (1996) Environmental health criteria 178 methomyl. World Health Organization, Geneva; see <http://www.inchem.org/documents/ehc/ehc/ehc178.htm>
- Tomar R (1997) Public health goal for OXAMYL in drinking water. Pesticide and environmental toxicology section, Office of Environmental Health Hazard Assessment (OEHHA), California Environmental Protection Agency (Cal/EPA); See also http://www.oehha.ca.gov/water/phg/pdf/oxam2_c.pdf#search='Oxamyl'
- United States Department of Agriculture (USDA) (2005) Agricultural chemical usage – 2004 restricted use summary. see also <http://usda.mannlib.cornell.edu/usda/nass/AgriChemUsRestricted//2000s/2005/AgriChemUsRestricted-10-05-2005.pdf>
- U. S. Environmental Protection Agency (EPA) (2002) Atrazine, Bensulide, Diphenamid, Imazalil, 6-Methyl-1,3-dithiolo[4,5-b]quinoxalin-2-one, Phosphamidon S-Propyl dipropylthiocarbamate, and Trimethacarb; Tolerance Revocations. *Federal Register Environmental Documents* 67, 46888–46893; see also: <http://www.epa.gov/fedrgstr/EPA-PEST/2002/July/Day-17/p17870.htm>
- Wagenet LP, Lemley AT, Wagenet RJ (1984) A review of physical-chemical parameters related to the soil and groundwater fate of selected pesticides used in New York state: oxamyl.

- The Pesticide Management Education Program (PMEP), Cornell University; see <http://pmep.cce.cornell.edu/facts-slides-self/facts/pchemparams/gen-pubre-Oxamyl.html>
- Watanabe N, Horikoshi S, Suzuki K, Hidaka H, Serpone N (2003) Mechanistic inferences of the photocatalyzed oxidation of chlorinated phenoxyacetic acids by electro-spray mass spectral techniques and from calculated point charges and electron densities on all atoms. *New J Chem* 5:836–843
- Watanabe N, Horikoshi S, Kawasaki A, Hidaka H, Serpone N (2005) Formation of refractory ring-expanded triazine intermediates during the photocatalyzed mineralization of the endocrine disruptor amitrole and related triazole derivatives at UV-irradiated TiO₂/H₂O interfaces. *Environ Sci Technol* 39:2320–2326
- Zaki MH, Moran D, Harris D (1982) Pesticides in groundwater: the aldicarb story in Suffolk County, NY. *Am J Public Health* 72:1391–1395